

# Detection of Mental Task Related Activity in NIRS-BCI systems Using Dirichlet Energy over Graphs

Panagiotis C. Petrantonakis, *Member, IEEE* and Ioannis Kompatsiaris, *Senior Member, IEEE*

**Abstract**— Near Infrared Spectroscopy (NIRS)-based Brain Computer Interfaces (NIRS-BCI) rely mainly on the mean concentration changes and slope of the hemodynamic responses in separate recording channels to detect the mental-task related brain activity. Nevertheless, spatial patterns across the measurement channels are also present and should be taken into account for reliable evaluation of the aforementioned detection. In this work the Dirichlet Energy of NIRS signals over a graph is considered for the definition of a measure that would take into account the spatial NIRS features and would integrate the activity of multiple NIRS channels for robust mental task related activity detection. The application of the proposed measure on a real NIRS dataset demonstrates the efficiency of the proposed measure.

## I. INTRODUCTION

The last two decades significant advancements have been accomplished in the research field of Brain-Computer Interfaces [1]–[3]. A great volume of research has been devoted in developing novel methodologies for deciphering the brain activity for communication and rehabilitation systems [4]. Among the brain-imaging techniques that have been used for the realization of a BCI system, Near Infrared Spectroscopy (NIRS) has lately attracted great attention due to recent technological advancements on novel wireless and wearable recording devices [5], [6] that allow for non-invasive, portable and efficient BCI systems.

NIRS facilitates light source-detector pairs in the near-infrared-range (650-1000 nm wavelength) and recording channels between the source-detector pairs. The recording sites capture the metabolic response, i.e., the concentration changes of the chromophores oxyhemoglobin (oxy-Hb) and deoxyhemoglobin (deoxy-Hb) [7]–[9] with respect to functional brain activity during cognitive, visual, or motor tasks. Changes in concentration levels of oxy-Hb and deoxy-Hb during changes in activation levels of neuronal populations can be related to mental task-specific responses and, thus, used for the realization of BCI systems.

In the vast majority of the NIRS-BCI systems the task-related functional brain activity is detected by estimating the mean concentration change (CC) values of the oxy-Hb and deoxy-Hb signals or the respective slope (S) of the aforementioned changes during task execution as compared to relax stages of non-task execution [10]. Thus, dynamic responses of certain NIRS channels are assessed individually without taking into account spatial characteristics of the NIRS signals as expressed throughout the NIRS channel

Research supported by the European Union’s Horizon 2020 research grant MAMEM (grant agreement No 644780).

The authors are with the Information Technologies Institute, Centre for Research and Technology – Hellas (CERTH), GR 57001, Thessaloniki, Greece. (correspondence e-mail: ppetrant@iti.gr)..

montage. Moreover, it was recently shown that antagonistic patterns of oxy- and deoxy-Hb signals appear in different brain regions simultaneously during a mental arithmetic task [11]–[13]. Hence new methodologies that would incorporate the spatial divergence of mental task-related NIRS signals should be introduced.

In this work we introduce a novel approach for detecting mental arithmetic task-related brain activity from NIRS signals by exploiting the notions of the emerging field of Graph Signal Processing (GSP). GSP theory [14]–[16] aims at analyzing high dimensional signals using graphs and expand traditional signal processing techniques to the graph-network domain. Recently various studies have used graph theory techniques for the analysis of brain activity [17]–[20]. In this study, the montage of NIRS channels is used to define the corresponding graph for analysis, where measurement channels correspond to graph vertices. The Dirichlet energy of the graph [14], [21] is used to capture the spatial divergence of the NIRS signals before and after a mental arithmetic task cue onset. The contribution of the proposed approach beyond the state of the art methodologies lies in the determination of a measure that integrates the activity of all NIRS channels and incorporates the spatial notion of NIRS signal divergence across the different channels.

The following sections II–IV describe the materials and methods used in this work, present the results and conclude the work, respectively.

## II. MATERIALS AND METHODS

### A. NIRS dataset and preprocessing

The dataset used in this study is available online (<http://bncl-horizon-2020.eu/database/data-sets>) [12]. The dataset consists of eight subjects (three male and five female) of age  $26 \pm 2.8$  (mean $\pm$ SD) that showed spatial, antagonistic hemodynamic, mental arithmetic task-related patterns [12]. Subjects were instructed to perform a cue-guided mental arithmetic task, i.e., subtract sequentially a one-digit number from a two-digit one for 12 seconds after the cue onset. The 12-second, task-related period was followed by a 28-second rest period (for details see online dataset documentation). Thus, each trial lasted for 40 seconds. In this work each trial is comprised of a 10 second period before cue onset (relax) for task execution, a 12-sec period of task execution and a 18-sec non-task period (relax). Subjects 1-3 performed 18 trials whereas subjects 4-8 performed 24 trials of mental arithmetic task.

The light source-detector pairs consisted of 16 light detectors and 17 light sources resulting in a 52-channel grid (see Fig. 1). The distance between light-source and light detector was 3cm, whereas the lowest line of measurement

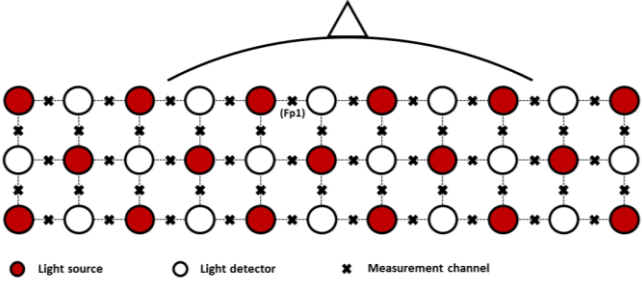


Fig. 1. Source-detector configuration. Red cycles represent light source whereas empty cycles represent light detectors. Source-detector distance is 3 cm. **X** symbol represents a measurement channel (Fp1 association with the measurement channels is illustrated).

channels was aligned with the Fp1-Fp2 line (Fp1 channel alignment is shown in Fig. 1). The sampling rate was 10 Hz.

An IIR bandpass filter of order 20 with cut off frequencies of 0.01Hz and 0.09Hz was used to remove the baseline drift and Mayer waves (~0.1Hz) [11]–[13]. Finally, the trial-related signal of all channels was referred to the 10-second baseline interval prior to the task.

### B. Graph and Graph Laplacian

Throughout this paper, a graph is defined as the pair  $\mathcal{G} = (\mathcal{V}, \mathcal{W})$  where  $\mathcal{V} = \{\mathbf{v}_1, \dots, \mathbf{v}_n\}$  is the set of  $n$  vertices and  $\mathcal{W} \in \mathbb{R}^{n \times n}$  is the adjacency matrix of the graph and  $w_{ij} \geq 0$  denoting the weight of the edge  $(i, j) \in \mathcal{E}$  (set of edges) between the vertices  $\mathbf{v}_i, \mathbf{v}_j \in \mathcal{V}$ . Graph  $\mathcal{G}$  is also considered to be symmetric, i.e.,  $\forall(i, j), w_{ij} = w_{ji}$ . The degree matrix  $D \in \mathbb{R}^{n \times n}$  of a graph is a diagonal matrix with diagonal elements  $D_{ii} = \sum_{j=1}^n w_{ij}, i = 1, \dots, n$ . Finally, the Laplacian matrix  $L \in \mathbb{R}^{n \times n}$  of a graph  $\mathcal{G}$  is defined as  $L = D - W$ . The Laplacian of a graph is a real, symmetric, positive semidefinite matrix.

### C. Graph Construction

For the estimation of the  $W$  matrix, the Semilocal (SL) approach was adopted as it was proved to be the most efficient among other approaches of  $W$  estimation for brain signals [19].

In a SL graph, only close NIRS measurement channels are connected (with the Euclidian notion of proximity) whereas the weights used correspond to the absolute value of covariance between the measurements of the two channels, i.e.,

$$W_{ij}^{cov} = \begin{cases} |cov(\mathbf{x}_i, \mathbf{x}_j)| & \text{if } d(\mathbf{v}_i, \mathbf{v}_j) \leq T_w \\ 0 & \text{otherwise} \end{cases} \quad (1)$$

where  $\mathbf{x}_i, \mathbf{x}_j$  are the graph signals that correspond to NIRS channels (vertices of the graph) for a specific trial of the task. A signal over a graph  $\mathcal{G}$  of the NIRS channels is a vector  $\mathbf{x} \in \mathbb{R}^n$  that is interpreted as scalar values observed in each vertex-channel  $\mathbf{v}_i \in \mathcal{V}, i = 1, \dots, n$ .  $d(\mathbf{v}_i, \mathbf{v}_j)$  is the Euclidean distance between the NIRS measurement channels-vertices (Fig. 1). Finally,  $T_w$  is the distance threshold that was used to determine the proximity threshold criterion.

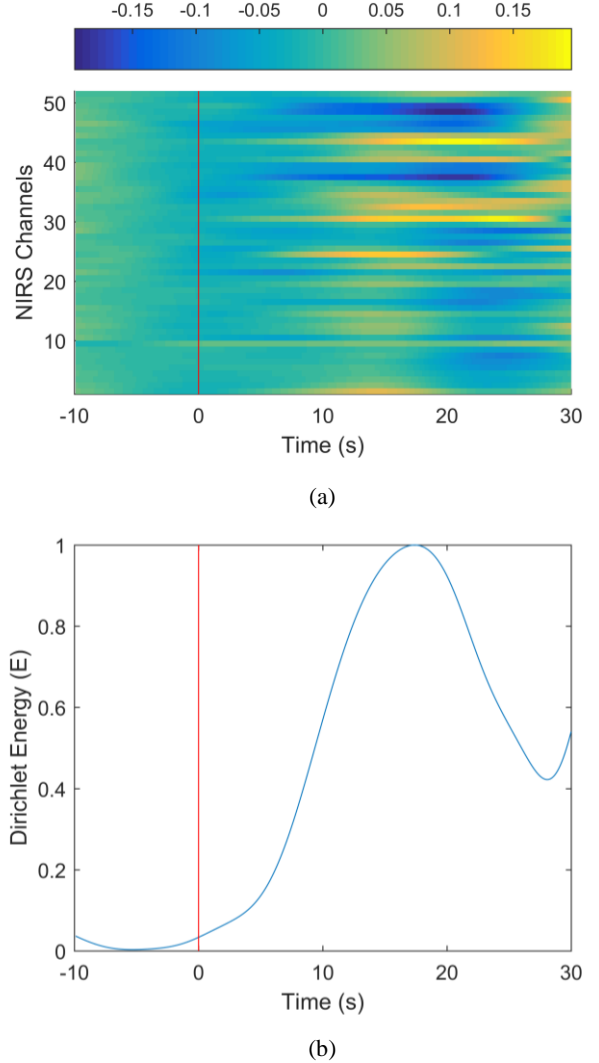


Fig. 2. (a) Concentration changes of oxy-Hb of trial=11 of subject 2 of each one of the 52 channels vs. time. (b) The estimated Dirichlet Energy (normalized in the range [0,1]) for the respective trial. Red vertical line corresponds to the cue onset.

After experimentation, we set  $T_w = 4.5$  cm. Furthermore, for the  $W^{cov}$  estimation the first two trials (approximately 10% of the trials) from each subject were used. The final  $W^{cov}$  resulted from the mean between the two trial-referred matrices. Finally, weights were normalized in the range [0, 1].

### D. Dirichlet Energy

In GSP theory the notion of smoothness of a graph signal  $\mathbf{x}$  is expressed via the  $p$ -Dirichlet form of  $\mathbf{x}$  which is defined as [14], [21]:

$$E_p(\mathbf{x}) = \frac{1}{p} \sum_{i \in \mathcal{V}} \|\nabla_i \mathbf{x}\|_2^p. \quad (2)$$

When  $p = 2$  then:

$$E_2(\mathbf{x}) = \sum_{(i,j) \in \mathcal{E}} w_{ij} (x_i - x_j)^2 = \mathbf{x}^T L \mathbf{x}, \quad (3)$$

that is, the graph laplacian quadratic form, which, throughout this work, will be denoted as the Dirichlet energy ( $E$ ) of  $\mathbf{x}$ . If

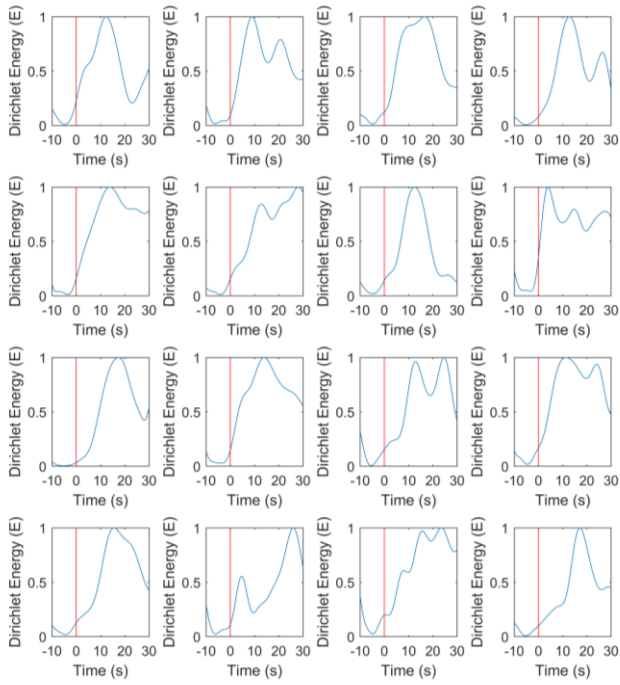


Fig. 3. The estimated Dirichlet Energy (normalized in the range [0,1]) measure for oxy-Hb for trials 3-18 of subject 2. Red vertical line corresponds to cue onset.

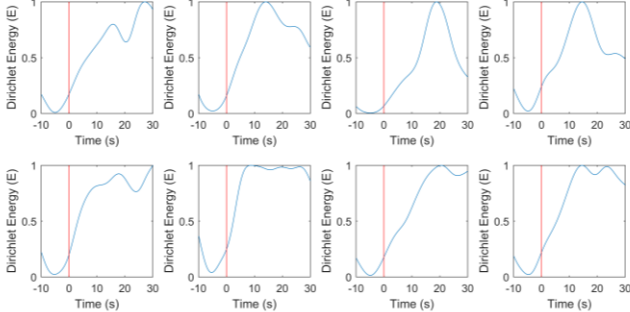
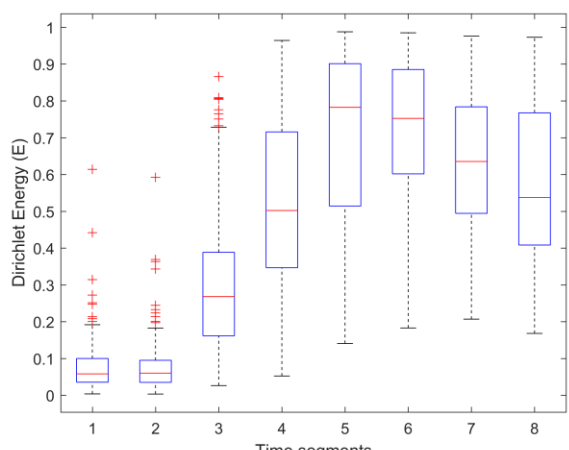


Fig. 4. The estimated mean Dirichlet Energy (normalized in the range [0,1]) measure for all trials of all eight subjects (upper left:subject 1, lower right:subject 8). Red vertical lines corresponds to cue onset.

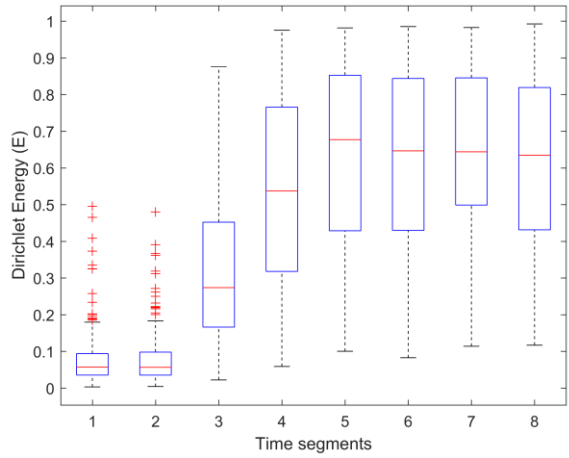
$\mathbf{x}$  is constant across all vertices of the graph then  $E = 0$ . In general  $E$  is small when the signal  $\mathbf{x}$  has similar values in neighboring vertices, i.e., the signal  $\mathbf{x}$  is smooth. In essence  $E$  is a measure of how much a graph signal changes with respect to the network. In the NIRS case it is a measure of how much a NIRS signal changes with respect to the channel montage. Thus, it is expected that  $E$  will be approximately zero when no mental-task is executed, thus no oxy-Hb or deoxy-Hb concentration changes are detected across NIRS channels. In the other hand  $E$  is expected to maximize within the task execution period.

### III. RESULTS

Figure 2 shows the concentrations changes of oxy-Hb for all NIRS channels across time (Fig. 2a) and the



(a)



(b)

Fig. 5. Boxplots of the Dirichlet Energy measure (normalized in the range [0,1]) for all trials of all eight subjects averaged within eight 5-second segments for (a) oxy-Hb and (b) deoxy-Hb.concentrations

corresponding  $E$  measure (Fig. 2b) for the respective mental arithmetic task trial of subject 2 of the dataset. Despite the fact that the graph NIRS signal  $\mathbf{x}$  is smooth during the pre-task period (10-sec period before red line) concentration changes start to vary after cue onset, leading to a more diverge texture of the graph signal. As expected, this spatial channel-oriented divergence is captured by the Dirichlet Energy measure which start to increase after the cue onset and decreases later on. It is noteworthy that despite the fact that the task execution period last for 12 seconds after cue onset, the spatial divergence last even after that time frame, entering the subsequent 18-second relax stage.

Figure 3 depicts the  $E$  measure for all task execution trials 3 to 18 (the first two trials are excluded as they were reserved for the estimation of graph weights, see Section II) of subject 2. Despite the fact that the Dirichlet Energy is maximized in different time bins during the mental task execution (or even after that) it is consistently very low during relax, pre-task period.

Figure 4 illustrates the mean Dirichlet Energy across all trials (3-18 for subjects 1-3 and 3-24 for subjects 4-8) for the oxy-Hb concentrations. Again, for all subjects the mean  $E$  measure across trials expresses the divergence of the NIRS signal that is exhibited during the mental task execution. Furthermore, it is noteworthy that during the pre-task 10-sec period, the  $E$  measure seem to decrease and increase, exhibiting a convex shape. The decrease part is due to the sequential realization of the trials resulting in having mental task execution before relax period and vice versa. Moreover, the part that  $E$  starts to escalate is shown to begin slightly before the cue onset. Probably, this is due to the fact that in each trial, before the cue onset for task execution there was an initial sign for trial initialization that would subconsciously lead to mental triggering. This may result in subsequent oxy-Hb concentration changes and thus escalation of the Dirichlet Energy.

In order to investigate if the mean  $E$  values differ significantly before and after the mental task cue onset, the whole trial duration was segmented in 8 parts and for each part the mean  $E$  value was estimated. Figure 5 illustrates the boxplots of these mean values for all trials of all subjects for oxy-Hb (Fig. 5a) and deoxy-Hb (Fig.5b). The 1-way anova analysis between all eight segments confirms that even within the first five seconds after onset (3<sup>rd</sup> time segment), the  $E$  values differ significantly from the corresponding segments before onset both for oxy-Hb and deoxy-Hb ( $p \ll 0.05$ ).

It should be stressed out that similar behavior of  $E$  measure as depicted in figures 2-4 is exhibited for concentration changes of deoxy-Hb. Thus,  $E$  measure seems to comprise a valuable tool for mental task related brain activity detection that integrates information from multiple channels in one measure and could be potentially used for the realization of NIRS-BCI systems. Further experimentation with the proposed measure is needed with more NIRS datasets and real BCI experimental settings.

#### IV. CONCLUSION

In this work a novel measure for the detection of the mental task related activity is presented. The proposed measure is based on the emerging field of GSP theory and exploits the Dirichlet Energy notion to capture the spatial divergence of the NIRS signal during mental task execution. The efficiency of the proposed measure is illustrated in real NIRS signals where it is shown to discriminate relax from task related periods even within a time frame of the first five seconds after onset. Nevertheless, the efficacy of the proposed approach should be further tested on more datasets for NIRS-BCI systems.

#### REFERENCES

- [1] I. Lazarou, S. Nikolopoulos, P. C. Petrantonakis, I. Kompatsiaris, and M. Tsolaki, "EEG-Based Brain–Computer Interfaces for Communication and Rehabilitation of People with Motor Impairment: A Novel Approach of the 21st Century," *Front. Hum. Neurosci.*, vol. 12, no. January, pp. 1–18, 2018.
- [2] U. Chaudhary, N. Birbaumer, and A. Ramos-murguialday, "Brain–computer interfaces for communication and rehabilitation," *Nat. Rev. Neurol.*, vol. 12, no. 9, 2016.
- [3] G. Schalk and E. C. Leuthardt, "Brain-computer interfaces using electrocorticographic signals," *IEEE Rev. Biomed. Eng.*, vol. 4, pp. 140–154, 2011.
- [4] M. A. Lebedev and M. A. L. Nicolelis, "Brain-Machine Interfaces: From Basic Science to Neuroprostheses and Neurorehabilitation," *Physiol. Rev.*, vol. 97, no. 2, pp. 767–837, 2017.
- [5] D. Wyser, O. Lambery, F. Scholkmann, M. Wolf, and R. Gassert, "Wearable and modular functional near-infrared spectroscopy instrument with multidistance measurements at four wavelengths," *Neurophotonics*, vol. 4, no. 4, p. 1, 2017.
- [6] A. von Lüthmann, C. Herff, D. Heger, and T. Schultz, "Toward a Wireless Open Source Instrument: Functional Near-infrared Spectroscopy in Mobile Neuroergonomics and BCI Applications," *Front. Hum. Neurosci.*, vol. 9, no. November, pp. 1–14, 2015.
- [7] F. Jobsis, "Noninvasive, infrared monitoring of cerebral and myocardial oxygen sufficiency and circulatory parameters," *Science (80.)*, vol. 198, no. 4323, pp. 1264–1267, 1977.
- [8] M. Ferrari and V. Quaresima, "A brief review on the history of human functional near-infrared spectroscopy (fNIRS) development and fields of application," *Neuroimage*, vol. 63, no. 2, pp. 921–935, 2012.
- [9] F. Scholkmann *et al.*, "A review on continuous wave functional near-infrared spectroscopy and imaging instrumentation and methodology," *Neuroimage*, vol. 85, pp. 6–27, 2014.
- [10] N. Naseer and K.-S. Hong, "fNIRS-based brain-computer interfaces: a review," *Front. Hum. Neurosci.*, vol. 9, no. January, 2015.
- [11] G. Bauernfeind, R. Scherer, G. Pfurtscheller, and C. Neuper, "Single-trial classification of antagonistic oxyhemoglobin responses during mental arithmetic," *Med. Biol. Eng. Comput.*, vol. 49, no. 9, pp. 979–984, 2011.
- [12] G. Pfurtscheller, G. Bauernfeind, S. C. Wriessnegger, and C. Neuper, "Focal frontal (de)oxygenated hemoglobin responses during simple arithmetic," *Int. J. Psychophysiol.*, vol. 76, no. 3, pp. 186–192, 2010.
- [13] G. Bauernfeind, D. Steyrl, C. Brunner, and G. R. Muller-Putz, "Single trial classification of fNIRS-based brain-computer interface mental arithmetic data: a comparison between different classifiers," *Conf. Proc. ... Annu. Int. Conf. IEEE Eng. Med. Biol. Soc. IEEE Eng. Med. Biol. Soc. Annu. Conf.*, vol. 2014, no. 288566, pp. 2004–2007, 2014.
- [14] D. I. Shuman, S. K. Narang, P. Frossard, A. Ortega, and P. Vandergheynst, "The Emerging Field of Signal Processing," no. may, pp. 83–98, 2013.
- [15] A. Sandryhaila and J. M. F. Moura, "Discrete Signal Processing on Graphs.pdf," *IEEE Trans. Signal Process.*, vol. 61, no. 7, pp. 1644–1656, 2013.
- [16] A. Sandryhaila and J. M. F. Moura, "Big data analysis with signal processing on graphs: Representation and processing of massive data sets with irregular structure," *IEEE Signal Process. Mag.*, vol. 31, no. 5, pp. 80–90, 2014.
- [17] W. Huang, L. Goldsberry, N. F. Wymbs, S. T. Grafton, D. S. Bassett, and A. Ribeiro, "Graph Frequency Analysis of Brain Signals," vol. 10, no. 7, pp. 1189–1203, 2015.
- [18] A. Y. Mutlu, E. Bernat, and S. Aviyente, "A signal-processing-based approach to time-varying graph analysis for dynamic brain network identification," *Comput. Math. Methods Med.*, vol. 2012, 2012.
- [19] M. Ménoret, N. Farrugia, B. Pasdeloup, and V. Gripon, "Evaluating Graph Signal Processing for Neuroimaging Through Classification and Dimensionality Reduction," 2017.
- [20] W. Huang, T. A. W. Bolton, J. D. Medaglia, D. S. Bassett, A. Ribeiro, and D. Van De Ville, "A Graph Signal Processing Perspective on Functional Brain Imaging," *Proc. IEEE*, pp. 1–18, 2018.
- [21] K. Smith *et al.*, "Locating Temporal Functional Dynamics of Visual Short-Term Memory Binding using Graph Modular Dirichlet Energy," *Sci. Rep.*, vol. 7, no. January, p. 42013, 2017.